

Article

# Feasibility Study on Grouting Compactness Detection in Sleeves Using Piezoelectric Transducers

Chen Wu <sup>1,2,\*</sup>, Chao Yang <sup>1,2</sup>, Shenglan Ma <sup>1,2</sup> and Xiaoliang Xu <sup>3</sup>

<sup>1</sup> School of Civil Engineering, Fujian University of Technology, Fuzhou 350118, China; ycfjut@163.com (C.Y.); mashenglan@fjut.edu.cn (S.M.)

<sup>2</sup> Fujian Provincial Key Laboratory of Advanced Technology and Informatization in Civil Engineering, Fuzhou 350118, China

<sup>3</sup> Tongji Architectural Design (Group) Co., Ltd., Shanghai 200092, China; 12XXL@tjad.cn

\* Correspondence: wuchen2001@126.com; Tel.: +86-1330-590-4530

Received: 25 November 2019; Accepted: 18 December 2019; Published: 23 December 2019



**Abstract:** Steel sleeve grouting connections are widely used in prefabricated concrete structures. It is well known that insufficient grouting increases the chance of structural failure. As such, it is critical to monitor the density and compactness of grouting sleeve during the construction process, which however remains significant challenges as it is deeply buried in the beam and column. In this study, a lead zirconate titanate (PZT)-based sleeve grouting compactness detection method was systematically investigated. Five grouting sleeves samples with different degrees of compactness were prepared and four PZT transducers were surface-bonded on opposite sides of the outer wall of each sleeve. Two acts as actuators to generate stress wave signals, and the other two operate as sensors to receive the signals. The wavelet packet energy and Hilbert–Huang transform methods were applied to process the stress wave signals, and with the chosen characteristic parameters, the correction model of the grouting compactness was established. Experimental results show that the wavelet packet total energy values and the Hilbert energy peak values are related to the grouting compactness, indicating the feasibility of using PZT sensors to detect the compactness of grouting sleeves.

**Keywords:** grouting sleeve; lead zirconate titanate (PZT); grouting compactness; wavelet packet energy (WPE); Hilbert–Huang transform (HHT)

## 1. Introduction

Grouting sleeve connection (GSC) technology plays a major role in prefabricated concrete (PC) structures, which are among the most important structures in the construction industry. With GSC technology, steel bars are inserted into both ends of a sleeve, and high-strength grouting materials are injected. The mechanical properties of connection joints depend on the bonding force between the grouting materials and two small steel bars, as well as that of the inner wall of the sleeve [1–5]. Therefore, the reliability of the joined bar heavily depends on the compactness of the grouting materials in the sleeves. However, improper design and construction processes of structural components often lead to insufficient grouting.

Because of the invisibility of the grouting sleeve inside the structure, nondestructive testing methods are used to determine the grouting compactness. For example, Nie et al. [6] demonstrated the feasibility of using an ultrasonic method for grouting compactness detection. Later on, Jiang and Cai [7] proposed an ultrasonic probability method based on the t-distribution. Experimental results showed that this improved method could reduce the detection of workloads and improve detection efficiency while maintaining the detection accuracy. Li et al. [8] proposed an ultrasonic detection method based on wavelet packet energy for grouted defects in GSC, the results demonstrated that

the proposed method could effectively detect the grouted defects in a certain range. Liu et al. [9] identified insufficient grouting sleeves using the impact-echo method. In general, for single-row sleeves, the aforementioned methods provide fast qualitative analysis of the grouting quality. However, in many complex cases, e.g., where sleeves are arranged in double rows, the grouting quality in the GSC cannot be detected immediately. Thus, many scholars have focused on detecting the grouting quality in the GSC in PC structures. For instance, Gao et al. [10] used industrial X-ray computed tomography (X-CT) to test the grouting compactness of sleeves encased in both plain and reinforced concrete and to overcome the problem of interference from the steel bars, concrete, and sleeves. However, this method is only suitable for detecting parallel pieces and depends on the shielding conditions in the laboratory. Using X-ray digital radiography, Li et al. [11] studied the quality of the sleeve grouting of a precast shear wall. The experimental results showed that the proposed method was feasible for detecting the grouting compactness in both single-row and plum-pile arrangement sleeves. However, it requires extensive safety protection measures to prevent radiation, which limits the potential application of this technology.

In summary, existing detection methods for the grouting compactness of sleeves, as described in the current literature, have several problems. For instance, it can only determine whether there are grouting defects, but not the defect rate. In addition, the detection accuracy is low, and long-term detection is not possible.

Lead zirconate titanate (PZT), the most common piezoelectric materials, has been widely used in structural health monitoring (SHM) due to its low cost, high bandwidth, fast response, and dual capability of actuation and sensing [12,13]. PZT-based stress wave method is an advanced active energy harvesting and sensing testing method [14]. The propagation distance between stress waves in the structure is large, and the detection range is broad. Additionally, many types of excitation signals exist, and many signal characteristics can be analyzed by using different modalities. Therefore, this method has been used for integrity assessment, health monitoring, and damage detection in civil engineering. Roh et al. [15] first used a PZT transducer and proposed the stress wave method in structural health monitoring. PZTs embedded in a structure emit and receive stress waves according to the direct and inverse piezoelectric effects of the piezoelectric materials. Structural damage is detected by establishing the relationship between the piezoelectric wave signals and the structural working states. Song et al. [16,17] proposed the “smart aggregate,” which embed PZT pieces in marble to better adapt them to the high-salinity environment of concrete materials, and successfully applied it in the early-age strength monitoring of concrete, impact detection, and structural health monitoring.

In SHM methods, establishing damage index is essential for diagnosis and identification of time, location and extent of structural damage. The commonly used damage indexes are amplitude, frequency, wave velocity and so on. However, there is no direct correlation between the damage of some structures and these indexes, and damage cannot be accurately described. Therefore, the signal processing method is vital, and wavelet packet energy (WPE) [18] method and Hilbert-Huang transform (HHT) [19] method are common signal processing methods. Jiang et al. [20] presented a stress wave-based method to detect the crack in FRP-reinforced concrete beams. The research validated damage characteristics extracted in PZT signal by the WPE method were able to effectively monitor the crack occurrence and development. Xu et al. [21,22] employed the stress wave method for monitoring the debonding damage in concrete-filled steel tubes. Using the WPE method, the damage index, which is known as the weighted energy ratio variation, was defined and used effectively to monitor the damage zone between the steel and concrete. Hu et al. [23] investigated the nonlinear vibro-acoustic modulation technique for damage detection in metallic structures. PZT transducers were bonded on the surface of aluminum specimens. Instantaneous characteristics of the response were extracted from received signals by the HHT method and used for evaluating the damage location and degree of composite materials. Hong et al. [24] used the nonlinear ultrasonic modulation method with piezoceramic transducers to detect the debonding in hidden frame supported glass curtain walls. The received signals were processed by the HHT method and the characteristics component containing the nonlinear damage information

were selected. The experiments verified the feasibility and effectiveness of the nonlinear ultrasonic modulation method in debonding detection of hidden frame supported glass curtain walls.

Currently, stress wave methods using PZT detection technology to monitor the grouting compactness of ducts have been developed [25–27]. The WPE analytical method was adopted to compute the total signal energy using PZT sensors. The results showed that the wavelet packet total energy value reflected the degree of grouting in the duct [25,27]. However, the inner diameter of the tendon duct is usually greater than 50 mm, while the inner diameter of the grouting sleeve is generally less than 50 mm. Therefore, the internal environment of the sleeve is more complicated than that of the duct. As such, the influence of steel in the grouting sleeve cannot be ignored.

At present, there is no method to complete the detection of sleeve grouting compactness at a low cost, and the detection of the sleeve in a double-row arrangement cannot be realized. PZT based detection has certain advantages in two aspects. In this paper, a stress-wave-based active sensing approach was adopted to detect the grouting compactness of sleeves. In the proposed method, PZT pieces covered in epoxy resin are attached to the opposite sides of the outside surface of a sleeve, and the sleeve is pre-filled with grouting materials. Fifteen samples with different grout degrees ranging from 0% to 100% grouting were experimentally studied. The WPE and HHT methods were used to analyze the signals received from PZT sensors. The compactness detection results showed that the degree of grouting significantly affected the propagation of the stress wave; thus, the relationship between the two was established. And the effectiveness of the proposed PZT-based method was demonstrated.

## 2. Detection Method of Piezoceramic Transducer

### 2.1. Piezoelectric Effect

Crystal materials having a piezoelectric effect are known as piezoelectric materials. When piezoelectric materials are subjected to an external load, the positive and negative charges inside the materials do not coincide and are expressed as charges on the surface of the materials. This phenomenon is called the direct piezoelectric effect and is illustrated in Figure 1a. The opposite effect is called the inverse piezoelectric effect [25], as shown in Figure 1b.

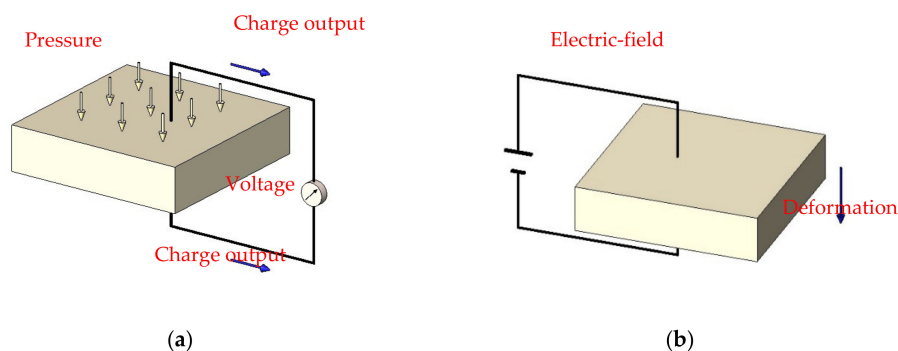


**Figure 1.** Piezoelectric effect: (a) conversion of pressure into voltage difference; (b) conversion of voltage into deformation.

### 2.2. Wavelet Packet Energy Method

For small cracks, the stress waves may be diffracted and even transmitted directly. As the increase of crack sizes and widths, as well as the number of cracks, the scattering effect becomes apparent, and the energy of the stress wave signal is attenuated. According to the definition of the WPE, the original signal  $S$  received by the PZT sensor is decomposed by the  $N$ -layer -wavelet packet to obtain  $2^N$  sub-signals [21,22].  $S$  can be expressed as follows:

$$S = s_1 + s_2 + s_3 + \cdots + s_{2N-1} + s_{2N} \quad (1)$$

where  $s_1 - s_{2N}$  are the wavelet coefficient bands in the final stage.

The variable  $s$  can be expressed as

$$s = [x_1, x_2, x_3 \cdots x_m], \quad (2)$$

where  $x$  is the amplitude of each band, and  $m$  is the number of sampling points.

The energy of each frequency band  $e$  is defined as

$$e = x_1^2 + x_2^2 + x_3^2 + \cdots + x_m^2. \quad (3)$$

The total energy  $E$  is expressed as

$$E = \sum e_i, \quad (4)$$

where  $i$  is the number of frequency bands ( $i = 1 \dots 2^N$ ).

Equation (4) can be used to analyze the grouting compactness in the time domain.

### 2.3. Hilbert-Huang Transform Method

The HHT is a signal time-frequency processing method [19]. In the HHT, the intrinsic mode function (IMF) obtained via empirical mode decomposition (EMD) reflects the inherent physical characteristics of the original data. Compared with the wavelet packet energy method, a basis function is not required. However, each IMF must meet the following conditions: (1) the sum of the positive and negative values of the function must be the same as the zero-crossing point, or at most, they differ by one; (2) the upper and lower envelopes formed by the extreme values have an average value of zero [28]. The HHT can adaptively localize the signal from the characteristic time scale of the non-stationary signal. The acquired piezoelectric signal is transformed to depict its Hilbert energy spectrum, where the energy accumulated by each frequency is expressed over the entire length of time [29,30]. In addition, the Hilbert energy is more concentrated than the wavelet energy.

The Hilbert amplitude spectrum  $H(\omega, t)$  is obtained by applying the Hilbert transform to each IMF component after EMD, as follows:

$$H(\omega, t) = \text{Re} \sum_j^n a_j(t) e^{i \int \omega_j(t) dt} \quad (5)$$

where  $\text{Re}$  is the real part of the complex number, and  $a_j(t)$  and  $\omega_j(t)$  are the instantaneous amplitude and instantaneous frequency, respectively, of the  $j$ th IMF component.

The Hilbert energy  $ES(\omega)$  is defined by the following equation, in terms of the square of the amplitude-versus-time integral, which expresses the energy accumulated for each frequency over the entire length of time.

$$ES(\omega) = \int_0^T H^2(\omega, t) dt \quad (6)$$

Here,  $T$  is the length of time of the signal.

## 3. Experimental Setup

### 3.1. Specimen Fabrication

In the test for the grouting compactness detection of sleeves, the grouting compactness was controlled by the cavity areas of the rubber plugs, as shown in Figure 2a. The rubber plugs were placed at the ends of the sleeve and then the grouting material was poured. Excess grouting material flowed out from the notch of the rubber plugs to control the compactness, as shown in Figure 2b. The PZT patch used in this experiment is type PZT-5, with a size of  $8 \times 6$  mm and a thickness of 1 mm. The material properties of the PZT are shown in Table 1. To ensure that the PZT transducers operated

normally without being affected by the external environment, they were completely encapsulated with epoxy resin in the metal ring to protect them and the connecting wires, as shown in Figure 3. The schematic of the specimen is shown in Figure 4. Four transducers (i.e., actuator and sensor) were bonded to a predetermined position on the outer surface of the sleeve with epoxy resin to form two pairs of transmitting-receiving groups (i.e., A1S1 and A2S2). The distance between sensors and set screw were set as 80 mm. The length of the sleeves was 380 mm, and the diameter and thickness of the tendon duct were 51 and 4.5 mm, respectively. The length and diameter of the steel bars were 400 and 20 mm, respectively. During the experiment, the grout inlet and outlet of the sleeve were fixed with the ground; the ends of the steel bars were free. Three groups of 15 sleeve specimens were prepared in total. The cement used for grouting in this study was a high-strength micro-expansion grouting material specifically used in sleeve grouting connections. At the beginning of the study, the material properties of the grout were tested. The performance indices are presented in Table 2. The results satisfied the requirements of the code [31].



**Figure 2.** Settings of the grouting density: (a) cut rubber plugs; (b) sleeve locations where the grouting flowed out.

**Table 1.** Material properties of type PZT-5.

Type	Density (g/cm <sup>3</sup> )	Coupling Factor	Dielectric Constant	Dielectric Loss	Piezoelectric Coefficient	Curie Temperature (°C)	Mechanical Quality Factor
PZT-5	7.6	0.62	2200	2	500	270	80

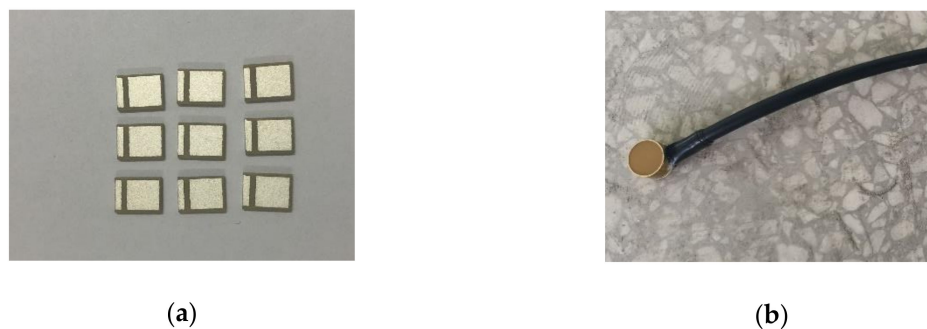


**Figure 3.** (a) PZT patches; (b) epoxy-resin-wrapped PZT patches.

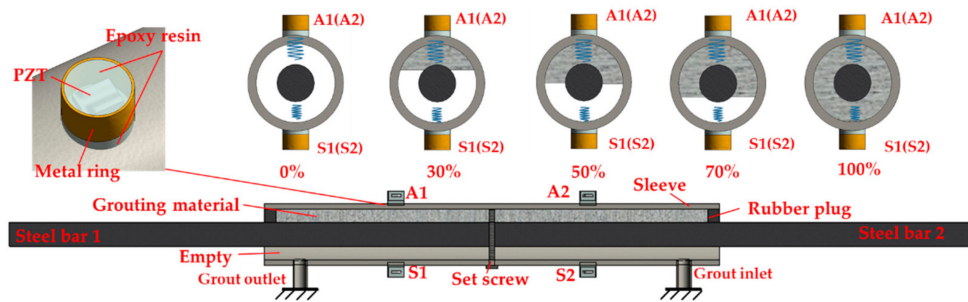


Figure 4. Schematic of the test specimen.

Table 2. Specifications for the grouting material characteristic experiment.

Tested Property	Performance Index		Measured Value
Fluidity/mm	Initial	≥300	355
	30 min	≥260	306
	1 d	≥35	58.5
Compressive strength/MPa	3 d	≥60	90.7
	28 d	≥85	122.2
Rate of upright direction expansion/%	Difference between 24 and 3 h	≥0.02	0.683
		0.02–0.5	0.225

### 3.2. Grouting Compactness Detection of Sleeves

After 28 d, the sleeve grouting compactness experiment was conducted. As shown in Figure 5, the experimental instruments included a real-time data acquisition system (NI-USB 6363), a single specimen, a voltage amplifier and a laptop with the LabVIEW software installed. Excitation signals were applied to the PZT-based actuator using the LabVIEW program to generate stress waves. Additionally, the signal response of each PZT sensor was recorded. The excitation signals were sine sweep signal. It was found that the signal energy was concentrated at 50 kHz–100 kHz by pre-scanning before the test began, while the signal energy was lower when it was out of range of 50 kHz–100 kHz, making it difficult to correlate with the grouting compactness of sleeve. Therefore, the frequency range of the test was set as 50 kHz–100 kHz. In order to increase the accuracy of the original signal obtained from the PZT sensor, each specimen was scanned for 5 consecutive times. Therein, each interval time and collection time were set as 10 s and 1 s, respectively. In addition, the amplitude of the signal was 10 V. The sampling frequency of each channel was 1 MHz. The voltage amplifier amplifies by 10 times.

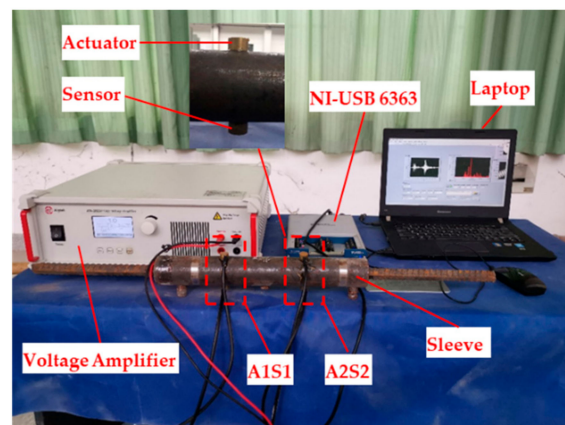


Figure 5. Experimental setup.

### 4. Test Results and Discussion

#### 4.1. Preliminary Processing of Signals

In order to reduce the influence of noise, the first and last signals were removed and the average value of the remaining three signals was taken as the original signal. In addition, for the sake of reducing the interference of noise, the wavelet transform was used to denoise. Therein, wavelet basis function was sym8 and the decomposition layer was set as four. The preliminary processing results are shown in Figure 6.

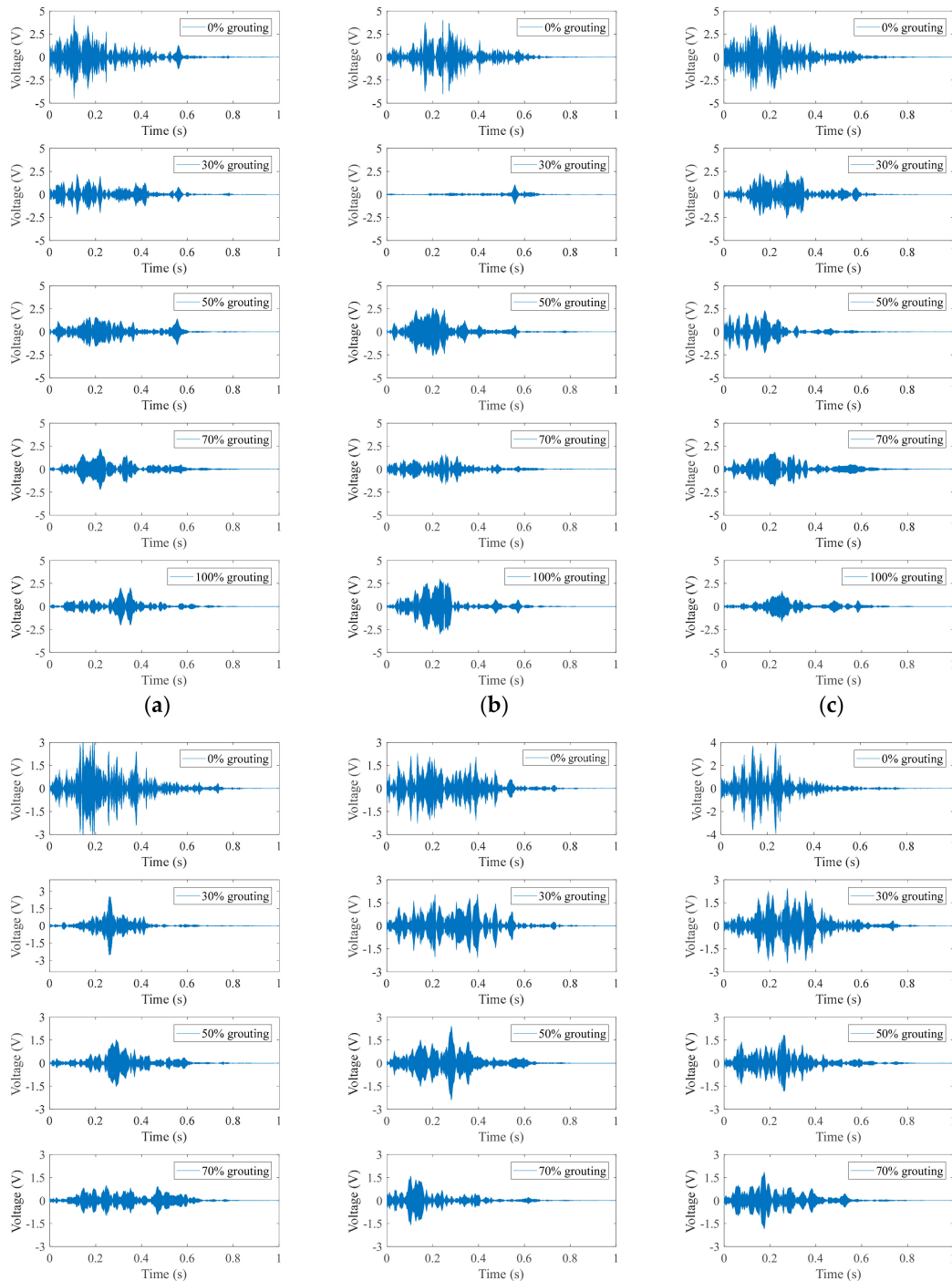
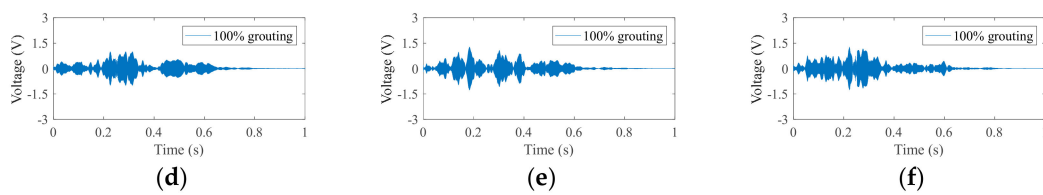


Figure 6. Cont.



**Figure 6.** Sine sweep signals of PZT sensors for different grouting compactness values: (a) 1st group of A1S1; (b) 2nd group of A1S1; (c) 3rd group of A1S1; (d) 1st group of A2S2; (e) 2nd group of A2S2; (f) 3rd group of A2S2.

4.2. Grouting Compactness Detection Based on WPE Method

For WPE, both the wavelet basis and decomposition layer may affect the detection result [32]. The results obtained by using different wavelet bases for the same signal are often quite different. In addition, the number of decomposition layers is too small and the denoising effect is not ideal, while too large decomposition layers will lead to the increase of computation and serious information loss. In this paper, since wavelet basis sym8 has the characteristics of compact support set, good continuity, and symmetry, sym8 is used to identify grouting compactness by trials. In terms of the decomposition layer, when the decomposition layer was set as five, the fifth layer signal had serious information loss. Therefore, in sym8, the decomposition layer was set as four.

4.3. Grouting Compactness Detection Based on HHT Method

The process of HHT is as follows: firstly, EMD method is used to decompose the preliminary processing signal into several IMF components based on the screening conditions of IMF; Then, Hilbert transform is performed for each IMF to obtain corresponding Hilbert spectrum. Therein, the Hilbert spectrum of all IMF is superimposed to obtain a Hilbert spectrum of the original signal. Finally, the amplitude square of the Hilbert spectrum is calculated as the Hilbert energy spectrum, which is used to detect the grouting compactness. The process diagram of the Hilbert-Huang conversion process is shown in Figure 7.

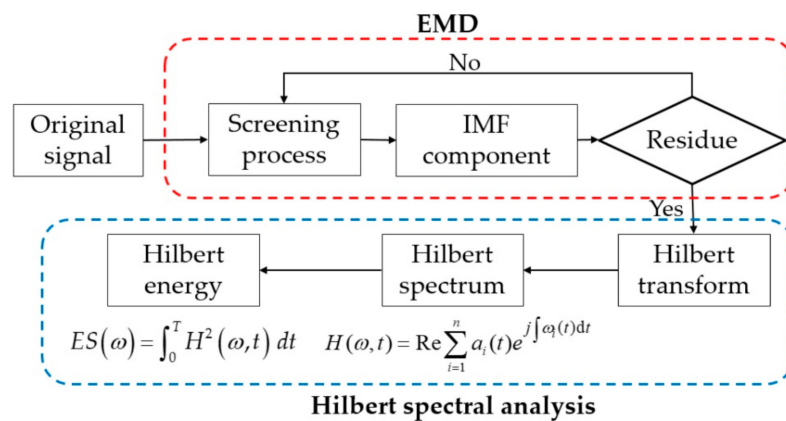


**Figure 7.** The process diagram of the Hilbert–Huang conversion process.

4.4. Grouting Compactness Detection Result and Discussion

The wavelet packet total energy values (WPTEVs) and Hilbert energy peak values (HEPVs) for the 15 specimens are presented in Table 3. It can be seen from Table 3 that the WPTEV and HEPV both showed a rising trend with the decrease of grouting compactness. It is indicated that the energy of the stress wave was decreased when the grouting gradually became full. However, the 2nd group of A1S1 in 30% and 100% grouting compactness both showed as the abnormal values. Possible reasons were the unavoidable human or external conditions such as uncontrolled grouting and the different thicknesses of the epoxy.

**Table 3.** Grouting-compactness indices.

Methods		WPTEVs					HEPVs				
Grouting compactness of sleeve		0%	30%	50%	70%	100%	0%	30%	50%	70%	100%
Serial Number	1st group of A1S1	663.23	388.93	388.43	388.60	325.43	0.154	0.0485	0.0551	0.0641	0.0439
	2nd group of A1S1	611.60	111.81	533.27	303.12	577.06	0.163	0.0013	0.1200	0.0358	0.1500
	3rd group of A1S1	714.09	510.44	418.36	400.41	288.51	0.196	0.114	0.0616	0.0645	0.0350
	1st group of A2S2	549.37	314.57	259.85	240.05	234.02	0.122	0.0452	0.0283	0.0194	0.0188
	2nd group of A2S2	455.73	435.46	382.89	254.81	250.92	0.072	0.0666	0.0625	0.0212	0.0207
	3rd group of A2S2	567.11	481.14	336.66	306.49	259.84	0.126	0.0897	0.0443	0.0357	0.0266

The relationship between the values of the grouting compactness and the proposed indices was established, as shown in Figure 8. The WPTEV and HEPV measured via the WPE and HHT methods, respectively, clearly exhibited relationships with the grouting compactness. With the increase of grout compactness, the compactness index signatures decrease, indicating that both signal-processing methods can be used for detecting the sleeve grouting compactness.

From the comparison of two methods, it was found that with the increasing of grouting compactness, both WPTEV and HEPV declined. However, the decreasing ratio of HEPV is slightly larger than that of WPTEV. It was indicated that both methods were able to detect grouting compactness, compared with the WPE method, the HHT method better reflected the relationship between the density and the piezoelectric signal index. Moreover, compared with the WPE method, the HHT method did not consider basis functions or the level number of decompositions. As a result, the authors recommend using the HHT method to detect grouting compactness.

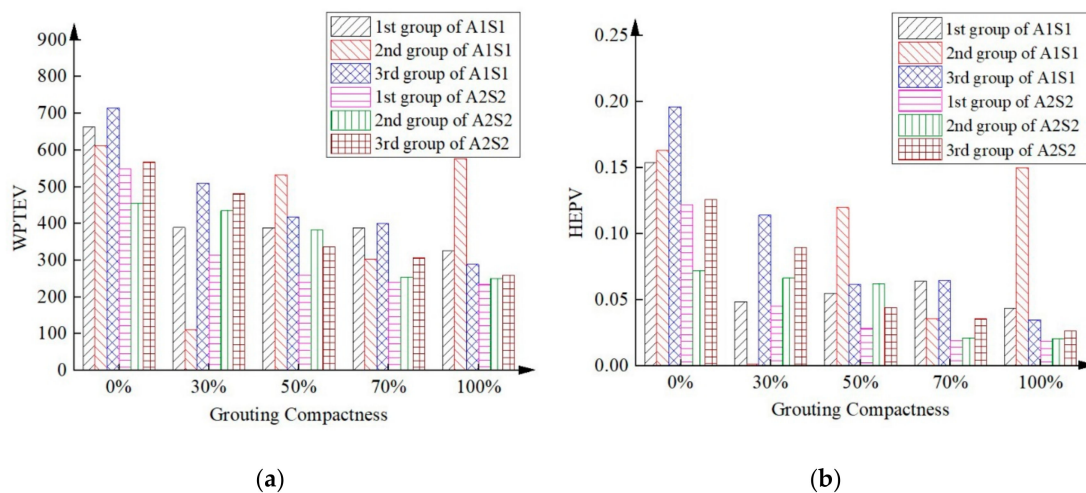


**Figure 8.** Relationship between the grouting compactness and the proposed indices: (a) wavelet packet energy (WPE) method, (b) Hilbert–Huang transform (HHT) method.

### 5. Conclusion and Future Work

Sleeve grouting compactness is a key factor in ensuring the performance of nodes in prefabricated concrete structures. Because the sleeve is invisible in the structure and thus not easily examined, only the slurry discharge state of the outlet hole of the mud has been used as a standard for grouting compaction, which is not a reliable method to indicate the compactness of sleeve grouting. Herein, a PZT-based detection method was proposed for monitoring the grouting compactness of sleeves in PC structures. The proposed method employs a stress-wave-based active sensing approach using PZT transducers. In the experiment, PZT transducers acting as an actuator and a sensor were bonded to opposite sides of a sleeve along the outer surface of the ring. The transducers were wrapped in epoxy resin to prevent the effects of the external environment. The WPE and HHT signal processing methods were used to analyze the signals received by the PZT sensor. Five grouting stages were

studied experimentally in the grouting range of 0% to 100%. The experimental results revealed that the signal index recorded by the PZT transducer decreases with respect to the grouting compactness, proving the feasibility of the method. The HHT method was more suitable than the WPE method on the grouting compactness detection in sleeves.

Compared with the existing sleeve compactness detection methods, the PZT-based method is not affected by the double-row arrangement of the sleeve and is more practical to be used in the field than the X-CT or X-ray methods. Although the proposed method is effective for detecting the grouting compactness, further quantitative investigations are required to establish correlations between WPTEV and HEPV signals and grouting compactness. Furthermore, future work should also focus on boundary conditions that affect results and detection of the grouting compactness of the sleeve inside the component under stress. Nevertheless, this study has demonstrated the feasibility of using PZT sensors to detect grouting compactness, and it lays a solid foundation for future studies.

**Author Contributions:** Conceptualization, C.W. and S.M.; provision of sensing technologies, X.X.; design of experiments, C.W. and C.Y.; execution of experiments and analysis of data, C.Y., C.W., and S.M.; writing of manuscript, C.Y.; revision of manuscript, C.W. All authors have read and agreed to the published version of the manuscript.

**Funding:** This work was supported by the National Natural Science Foundation of China with grant No. 51808119; the Fujian Industry-university Cooperation Project with grant No. 2019Y4011; the Fujian New Century Excellent Talent Support Project with grant No. GYZ-160144; and the Fujian University of Technology Research and Development Fund with grant No. GYZ-160126.

**Conflicts of Interest:** The authors declare no conflicts of interest.

## References

1. Ling, J.H.; Rahman, A.B.A.; Ibrahim, I.S.; Hamid, Z.A. Tensile capacity of grouted splice sleeves. *Eng. Struct.* **2016**, *111*, 285–296. [[CrossRef](#)]
2. Ling, J.H.; Rahman, A.B.A.; Ibrahim, I.S.; Hamid, Z.A. Behavior of grouted pipe splice under incremental tensile load. *Constr. Build. Mater.* **2012**, *33*, 90–98. [[CrossRef](#)]
3. Sayadi, A.A.; Rahman, A.B.A.; Jumaat, M.Z.B.; Johnson, A.U.; Ahmad, S. The relationship between interlocking mechanism and bond strength in elastic and inelastic segment of splice sleeve. *Constr. Build. Mater.* **2014**, *55*, 227–237. [[CrossRef](#)]
4. Xu, F.; Wang, K.; Wang, S.G.; Li, W.W.; Liu, W.Q.; Du, D.S. Experimental bond behavior of deformed rebars in half-grouted sleeve connections with insufficient grouting defect. *Constr. Build. Mater.* **2018**, *185*, 264–274. [[CrossRef](#)]
5. Kim, H. Bond strength of mortar-filled steel pipe splices reflecting confining effect. *J. Asian Archit. Build. Eng.* **2012**, *11*, 125–132. [[CrossRef](#)]
6. Nie, D.L.; Jia, L.G.; Du, M.K.; Liu, M. Experimental study on detecting density of grouting materials for steel sleeves by using ultrasonic wave. *Concrete* **2014**, *9*, 120–123.
7. Jiang, S.F.; Cai, W.X. Ultrasonic testing method of grouting sleeve compactness. *J. Vib. Shock*. **2018**, *37*, 43–49.
8. Li, Z.H.; Zheng, L.L.; Chen, C.J.; Long, Z.L.; Wang, Y. Ultrasonic Detection Method for Grouted Defects in Grouted Splice Sleeve Connector Based on Wavelet Pack Energy. *Sensors* **2019**, *19*, 1642. [[CrossRef](#)]
9. Liu, Y.L.; Wei, G.S.; Liu, Z.H.; Chen, X.D.; Wang, X.J. Detection of prefabricated shear wall grouting anchor grouting compactness based on the impact echo method. *J. Yangtze U. (Nat. Sci. Ed.)* **2017**, *14*, 26–31.
10. Gao, R.D.; Li, X.M.; Zhang, F.W.; Xu, Q.F.; Wang, Z.L.; Liu, H. Experiment on detection of coupler grouting compactness based on industrial X-CT. *Nondestruct. Test.* **2017**, *4*, 12–17.
11. Li, X.M.; Gao, R.D.; Xu, Q.F.; Wang, Z.L.; Zhang, F.W.; Xie, Y. Study on inspection technology for sleeve grouting connection quality of precast shear wall based on X-ray digital radiography method. *Build. Struct.* **2018**, *48*, 57–61.
12. Ghafari, E.; Yuan, Y.; Wu, C.; Nantung, T.; Lu, N. Evaluation the compressive strength of the cement paste blended with supplementary cementitious materials using a piezoelectric-based sensor. *Constr. Build. Mater.* **2018**, *171*, 504–510. [[CrossRef](#)]

13. Su, Y.; Han, G.S.; Amran, A.; Nantung, T.; Lu, N. Instantaneous monitoring the early age properties of cementitious materials using PZT-based electromechanical impedance (EMI) technique. *Constr. Build. Mater.* **2019**, *225*, 340–347. [[CrossRef](#)]
14. Su, Y.; Kotian, R.R.; Lu, N. Energy harvesting potential of bendable concrete using polymer based piezoelectric generator. *Compos. Part B Eng.* **2018**, *153*, 124–129. [[CrossRef](#)]
15. Roh, Y.S. Built in Diagnostics for Identifying an Anomaly in Plates Using Wave Scattering. Ph.D. Thesis, Stanford University, Palo Alto, CA, USA, 1999.
16. Song, G.; Gu, H.; Mo, Y.L. Concrete structural health monitoring using embedded piezoceramic transducers. *Smart Mater. Struct.* **2007**, *16*, 959–968. [[CrossRef](#)]
17. Song, G.; Gu, H.; Mo, Y.L. Smart aggregate: Multi-functional sensors for concrete structures—a tutorial and review. *Smart Mater. Struct.* **2008**, *17*, 033001. [[CrossRef](#)]
18. Yen, G.G.; Lin, K.C. Wavelet packet feature extraction for vibration monitoring. *IEEE Trans. Ind. Electron.* **2000**, *47*, 650–667. [[CrossRef](#)]
19. Huang, N.E.; Shen, Z.; Long, S.R.; Wu, M.C.; Shih, H.H.; Zheng, Q.; Yen, N.C.; Tung, C.C.; Liu, H.H. The empirical mode decomposition and the Hilbert spectrum for nonlinear and non-stationary time series analysis. *Proc. R. Soc. A* **1998**, *454*, 903–995. [[CrossRef](#)]
20. Jiang, T.Y.; Hong, Y.; Zheng, J.B.; Wang, L.; Gu, H.C. Crack Detection of FRP-Reinforced Concrete Beam Using Embedded Piezoceramic Smart Aggregates. *Sensors* **2019**, *19*, 1979. [[CrossRef](#)]
21. Xu, B.; Li, B.; Song, G.B. Active debonding detection for large rectangular CFSTs based on wavelet packet energy spectrum with piezoceramics. *J. Struct. Eng.* **2012**, *139*, 1435–1443. [[CrossRef](#)]
22. Xu, B.; Zhang, T.; Song, G.; Gu, H.C. Active interface debonding detection of a concrete-filled steel tube with piezoelectric technologies using wavelet packet analysis. *Mech. Syst. Signal. Process.* **2013**, *36*, 7–17. [[CrossRef](#)]
23. Hu, H.F.; Staszewski, W.J.; Hu, N.Q.; Jenal, R.B.; Qin, G.J. Crack detection using nonlinear acoustics and piezoceramic transducers—instantaneous amplitude and frequency analysis. *Smart Mater. Struct.* **2010**, *19*, 065017. [[CrossRef](#)]
24. Hong, X.B.; Liu, Y.; Liufu, Y.H.; Lin, P.S. Debonding Detection in Hidden Frame Supported Glass Curtain Walls Using the Nonlinear Ultrasonic Modulation Method with Piezoceramic Transducers. *Sensors* **2018**, *18*, 2094. [[CrossRef](#)] [[PubMed](#)]
25. Jiang, T.Y.; Kong, Q.Z.; Wang, W.X.; Huo, L.S.; Song, G. Monitoring of grouting compactness in a post-tensioning tendon duct using piezoceramic transducers. *Sensors* **2016**, *16*, 1343. [[CrossRef](#)]
26. Jiang, T.Y.; Zheng, J.B.; Huo, L.S.; Song, G. Finite element analysis of grouting compactness monitoring in a post-tensioning tendon duct using piezoceramic transducers. *Sensors* **2017**, *17*, 2239. [[CrossRef](#)]
27. Xu, Y.; Luo, M.; Hei, C.; Song, G. Quantitative evaluation of compactness of concrete-filled fiber-reinforced polymer tubes using piezoceramic transducers and time difference of arrival. *Smart Mater. Struct.* **2018**, *27*, 035023. [[CrossRef](#)]
28. Leo, M.; Looney, D.; D’Orazio, T.; Mandic, D.P. Identification of Defective Areas in Composite Materials by Bivariate EMD Analysis of Ultrasound. *IEEE Trans. Instrum. Meas.* **2011**, *61*, 221–232. [[CrossRef](#)]
29. Wu, C.; Zhou, R.Z. Nonlinear behavior analysis of structural dynamic response based on Hilbert spectrum. *J. Vib. Shock* **2013**, *32*, 70–76.
30. Hong, X.B.; Liu, Y.; Lin, X.H.; Luo, Z.Q.; He, Z.W. Nonlinear ultrasonic detection method for delamination damage of lined anti-corrosion pipes using PZT transducers. *Appl. Sci.* **2018**, *8*, 2240. [[CrossRef](#)]
31. Standards Press of China. *JG/T 408-2013: Cementitious Grout for Coupler of Rebar Splicing*, Ministry of Housing and Urban-Rural Development of the People’s Republic of China; Standards Press of China: Beijing, China, 2013.
32. Sampath, S.; Bhattacharya, B.; Aryan, P.; Sohn, H. A Real-Time, Non-Contact Method for In-Line Inspection of Oil and Gas Pipelines Using Optical Sensor Array. *Sensors* **2019**, *19*, 3615. [[CrossRef](#)]

